Investigation of Control Surface Geometry on Hydrodynamic Performance

T. E. Ellis
Virginia Polytechnic Institute and State University,
Human Powered Submarine. (HPS)
Final Report

May 12, 2020

Abstract

Hydrodynamic forces placed on control surfaces allow submarines to maneuver and react to perturbations encountered during travel. As can be imagined, the geometric parameters around which these surfaces are designed greatly impact their maneuvering performance. This report seeks to understand the implications of several geometric parameters which contribute to the hydrodynamic forces placed on control surfaces such as pivot location, actuation range, cross sectional shape and span geometry to design an appropriate control surface geometry for the 2021 HPS submarine Nautilus. The final control surface shaft location was determined as the airfoil quarter chord which is the center of pressure location for symmetric thin airfoils. The final control surface span geometry will remain within the reflection plane of the hull to avoid oncoming turbulent flow, the aspect ratio should be high to improve aerodynamic efficiency, and the taper ratio should be around 0.6-0.8 to improve lift at higher angles of attack. An Xfoil investigation on cross-section shapes revealed the NACA 0009 airfoil as having the best compromise between maximum and average lift to drag ratio over a range attack angles from 0-20 degrees. The NACA 0009 reaches a maximum L/D efficiency at 6 degrees and encounters a stall angle at 8 degrees, making the desired actuation range of the final control surface from 0-8 degrees.

Keywords— Control Surface, Hydrodynamics, Airfoils, Submarine, Design

Nomenclature

α, AOA Angle of Attack

ρ Density

c Chord length

Cd Coefficient of Lift

Cl Coefficient of Lift

Cm Moment Coefficient

HPS Human Powered Submarine

ISR International Submarine Races

L/D Lift to Drag Ratio

LE Leading Edge

M, Ma Mach Number

$m.a.c$ Mean Aerodynamic Center

Re Reynolds Number

TE Trailing Edge

VT Virginia Tech

Xtr_Bot x-location of flow transition along bottom of airfoil

Xtr_Top x-location of flow transition along top of airfoil

1 Introduction

The Human Powered Submarine (HPS) Team at Virginia Tech (VT) designs, builds, and races a human propelled submarine which competes at the biennial International Submarine Races (ISR) competition held in Carderock, MD. At the previous ISR 15 competition held in 2019, the VT HPS Team's competition submarine *Trident* experienced difficulty in maintaining directional stability. Any small disturbance to the submarine's heading proved difficult for the pilot to correct using the large high control authority control surfaces on the submarine, see Fig. 1 below. The large moments induced by the control surfaces caused *Trident* to take a non-linear course of travel which added distance and time to submarine's travelled race path and finish time. Hydrodynamic forces placed on control surfaces allow submarines to maneuver and react to perturbations encountered during travel. As can be imagined, the geometric parameters around which these surfaces are designed greatly impact their maneuvering performance. This report seeks to understand the implications of several geometric parameters which contribute to the hydrodynamic forces placed on control surfaces such as pivot location, actuation range, cross sectional shape and span geometry to design an appropriate control surface geometry for the 2021 HPS competition submarine *Nautilus*. The

motivation of this research is to formulate and justify the design a control surface geometry that will enhance the directional stability of *Nautilus* and allow the submarine to achieve a top speed of 8.5 knots at the 2021 ISR 16 competition to break the human powered submarine world record for top speed.

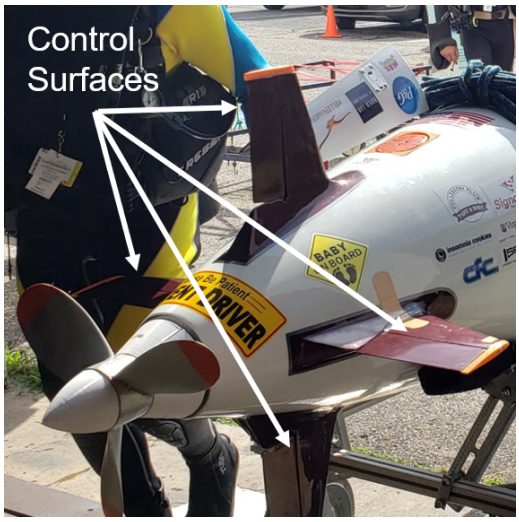

Figure 1: Aft view of *Trident* at ISR 15 showing the submarine's large control surfaces

To address this maneuverability problem faced by *Trident* at ISR 15, this control surface research is being divided into two main areas: sizing, and shape and geometry. This report is focused on the shape and geometry of the control surfaces, more specifically the hydrodynamic aspects which affect the geometric characteristics of a control surface. This research will be governed by an exploration to determine appropriate values for a control surface cross-sectional series, actuation rod location, aspect ratio and taper ratio. A determination for the final cross-sectional shape will be determined from an investigation into the hydrodynamic forces placed on various control surface cross sectional shapes analyzed using a program designed for the design and analysis of subsonic airfoils called Xfoil. The results collected from Xfoil will be used to mathematically justify the final control surface cross sectional shape for *Nautilus*. A verification of the results collected from Xfoil will then be compared to the collected results from other experiments and the final Xfoil determined cross section geometry will be compared to manufacturing design constraints.

1.1 Determination of Airfoil Series

Experiments have previously been conducted examining the effects of cross-sectional series shapes on control surface aerodynamic performance. In the research done by Abbot and Van Doenhoff presented in their book, *Theory of Wing Sections*, they list the test data collected from a wide range of NACA series airfoil sections. From Abbot and Van Doenhoff's experimental results, two airfoil series were decided to be evaluated as potentially viable cross-sectional series for *Nautilus* because of their low drag characteristics which make these series favorable for marine applications. These were the NACA 65 and 66 series and the NACA 00 series airfoils. Results from experiments conducted by Abbot and Van Doenhoff show the NACA 65 and 66 series airfoils as having low drag characteristics at low angles of attack, AOAs, specifically within 3 degrees of actuation. Because

of this high efficiency at a low range of actuation angles, these airfoils are commonly used in high speed applications where actuation angles are desired to be small to prevent drag. As the AOA of these airfoil series increase beyond 3 degrees, these airfoils experience an early flow separation, high drag, and early stall angle (Abbot and Van Doenhoff). The NACA 00 airfoil series was the second series evaluated. From Abbot and Van Doenhoff's data the NACA 00 series is suitable for a large variety of movable appendages such as rudders and control surfaces due to the efficient operation of this series over a wide range of angles.

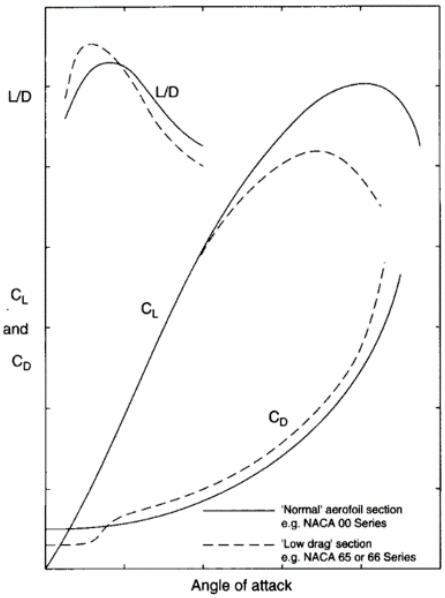

Figure 2: Comparison of NACA 00 and NACA 65 and 66 Series Performance Characteristics, *Theory of Wing Sections* (Abbot and Van Doenhoff)

Figure 2, above, plots the NACA 00 vs 65 and 66 series coefficients of lift, abbreviated Cl, coefficients of drag, abbreviated Cd, and lift over drag ratios, also known as aerodynamic efficiency and abbreviated as L/D, plotted against AOA from Abbot and Van Doenhoff experiments. The coefficients of lift and drag are used to denote the aerodynamic forces per unit span on a surface. This is done by non-dimensionalizing, which removes the relation of these forces to their sized dimensions. Since the forces are forces per unit span, these coefficients can also be used to compare and scale between different sized models.

Note that magnitudes on Fig.2 are not listed for AOA or Cl, Cd, or L/D which could due to privacy reasons. The graphic is still useful however in visually displaying the trends between the NACA 00 and NACA 65 and 66 series which show that for a large range of AOAs the NACA 00 series has a overall higher L/D, higher Cl, and lower Cd than the NACA 65 and 66 series airfoils. These trends support the observations of Abbot and Van Doenhoff, which mention the NACA 00 series as being more suitable for most vehicles which require movable appendages, such as rudders and control surfaces, due to the efficient operation of this series over a wider range of angles (Abbot and Van Doenhoff). Since *Nautilus* is not expected to travel at particularly high-speeds, it was decided that an airfoil from the NACA 00 series would be used for the control surface cross-section shape as it would allow the pilot some autonomy in the control surface actuation range.

1.2 Determination of Control Surface Shaft Location

Research into the aerodynamics on symmetric thin airfoils was also conducted to aid in justifying a placement location for the control surface actuating shaft. From experiments conducted by the National Aeronautics and Space Administration, NASA, it has been found both experimentally and theoretically that if the aerodynamic force is applied at a location 1/4 chord, on most low speed airfoils, the magnitude of the aerodynamic moment remains nearly constant with angle of attack. This 1/4 chord location on a thin symmetric airfoil is also known as the center of pressure.

The center of pressure develops from changes in AOA which create changes in pressure variations on airfoils. Figure 3, below, shows an example of a pressure distribution magnitude on the top and bottom surfaces of an arbitrary airfoil shape set at a 25 degree AOA where the pressure distribution can be seen marked on the figure by red lines. Averaging this red pressure distribution chordwise along the airfoil reveals the location of the center of pressure, shown as a yellow dot. At this location, the pressure forces are equal on either side of the airfoil horizontally from left to right. Between the top and bottom surfaces, an aerodynamic force develops from the uneven vertical pressure distribution on the airfoil as shown in dark blue. This aerodynamic force can be decomposed into a lift and drag force, L and D, shown in light blue. If the aerodynamic force is placed at the center of pressure, there is no aerodynamic moment or pitching moment, since the pressure forces are balanced from left to right on the airfoil. Therefore, it is desired that the control surface rod on *Nautilus* be at the center of pressure of the airfoil so that the moment generated by the control surface will remain constant at a near zero value despite changes in AOA. This will prevent the pilot of the sub from experiencing resistive torque which would make the control surfaces harder to actuate.

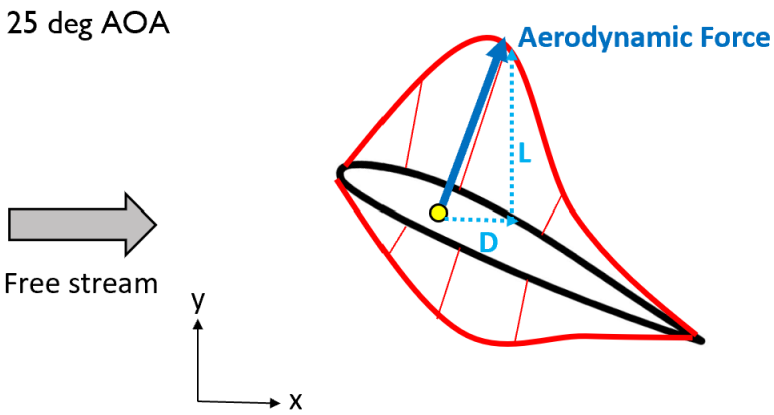

Figure 3: Depiction of a Pressure Distribution (red), Center of Pressure (yellow), and Aerodynamic Force (blue) placed on an Arbitrary Airfoil Profile at 25 Degrees

1.3 Comparison of Control Surface Characteristics

Other HPS design teams at the previous 2019 ISR competition also took geometry and hydrodynamics into consideration when designing their control surfaces. A submarine designed by the l'École de Technologie Supérieure which competed at ISR 15, OMER 11, placed 1st at competition

for the fastest submarine which registered at 6.85 knots. The team utilized a NACA 0009 airfoil as the section shape for both their horizontal and vertical control surfaces, see Fig.4 below. The team's rationale for choosing this airfoil shape was based on their desire to have the control surface thickness be as small as possible while still being able to house a 10 mm control rod shaft within the control surface's cross section (OMER 11). This airfoil is from the same series as the type chosen for *Nautilus*. Additionally the team determined that the control rod to actuate the control surface would be placed at the 41 percent chord location due to relative success in their previous years design (OMER 11).

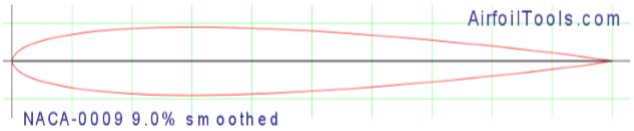

Figure 4: NACA 0009 Section Shape used by OMER 11 at ISR 15 (OMER 11)

WASUB IX, a submarine designed by Delft University of Technology and Vrije Universiteit Amsterdam, was the second fastest submarine at the ISR 2019 competition posting a time of 6.54 knots. This team also used a NACA 0009 airfoil for both their horizontal and vertical control surfaces but placed their rod to actuate the control surface at the 1/4 chord location to reduce resistive torque experienced when actuating the control surfaces (WASUB IX). This airfoil series and shaft location placement match with the airfoil series and shaft location placement research findings for *Nautilus*. Figure 5, below, shows the two vertical NACA 0009 cross section control surfaces from a CAD model of the WASUB IX submarine model raced at the ISR 15 competition.

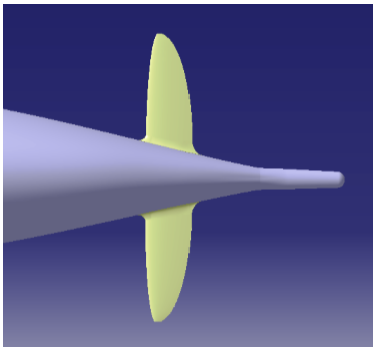

Figure 5: Vertical Control Surface Shape used by WASUB IX at ISR 15 (WASUB IX)

1.4 Determination of Control Surface Span Geometry

Research on control surface span geometry has also been conducted, examining the impacts of aspect ratio and taper ratios on control surface performance. In Molland and Turnock's book *Marine Rudders and Control Surfaces: Principles, Data, Design and Applications* they discuss that having high aspect ratio generally creates a more efficient rudder by reducing control surface's drag for a given lift. Examples of high aspect ratios are around 5-6 (Molland and Turnock), therefore to maximize aerodynamic efficiency the aspect ratio for *Nautilus* should be as close to 5-6 as possible. With regards to taper ratio, moderate taper ratios of 0.6-0.8 are recommended in order to produce elliptical loading on the planform area to induce less drag on the control surface (Molland and Turnock). To minimize induced drag on the control surfaces the taper ratio for *Nautilus* should

be as close to 0.6-0.8 as possible. Additionally, to prevent the rudder from coming into contact with the turbulent boundary layer of the hull, the span of the control surfaces for *Nautilus* should remain within the maximum diameter of the submarine otherwise referred to as the reflection plane (Molland and Turnock).

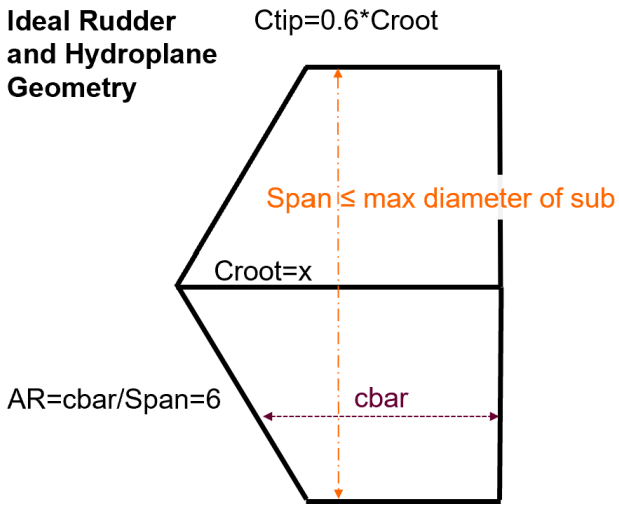

Figure 6: Vertical Control Surface Shape used by WASUB IX

Figure 6, above, displays an ideal rudder and hydroplane geometry, also known as the vertical and horizontal control surface geometry, based off the characteristics described in *Marine Rudders and Control Surfaces: Principles, Data, Design and Applications*. The aspect ratio equation is listed on the figure as being the average chord length, cbar, over the span length of the control surface, labelled in orange. It is also listed that the max span of the control surfaces should be within the maximum diameter of the submarine hull. The taper ratio, which is the chord tip length over the root chord length, Croot, has been accounted for in the calculation of Ctip on the diagram where the taper ratio has been set to 0.6 and the resulting chord tip length has appropriately been set to be 60 percent of the root chord length. The remainder of this report is organized in the following order: Methodology for Xfoil Investigation (which includes the sub-sections: Identification of Constraints, an overview of the Xfoil Investigation Procedure, and Comparison of Constraints), Results Presentation displaying the collected Xfoil data, Analysis of Results (consisting of the sub-sections Verification of Xfoil Results, and Visualization of Constraints which displays post-processed results), a Conclusion section reviewing the highlights of the results and analysis of results sections, and Future Work describing experimental improvements and uncertainties to be explored.

2 Methodology for Xfoil Investigation

2.1 Identification of Constraints

The control surface airfoil cross section investigation described in this report was conducted with consideration to both the physical design constraints set forth by the HPS controls group and the necessary input assumptions and constraints required to focus the scope of Xfoil airfoil performance investigation. To reduce some of the many variables which affect control surfaces, the HPS controls

group was asked to develop a list of soft and hard constraints that would guide the investigation moving towards the final control surface design. Soft constraints were considered values which may need to be revised or are capable of being modified based on the qualitative or quantitative results from research or the results from Xfoil airfoil performance tests. Hard constraints were defined as values which must remain constant throughout the design investigation, typically for fabrication reasons. The constraints are listed in table 1 below.

Table 1: Constraint Table

Table of Constraints			
Constraint	Value	Soft/Hard Constraint	Determined By
Moment Arm length from Submarine's Center of Gravity	1.05 m	Hard	HPS Controls Group
Actuating Rod Diameter	3/8 in	Hard	
Spacing around Actuating Rod Hole	1/8 - 1/4 in	Soft	
Maximum Angle of Actuation	15 degrees	Soft	Other
Mach Number	0	Hard	
Water Temperature At Carderock Basin	65 degrees F	Soft	

From table 1, the moment arm of the control surface which is the distance from the control surface shaft to the submarine's center of gravity was chosen as being 1.05 meters from the center of gravity, Cg. This value was determined from asking the controls group the furthest location aft they could feasibly fit the control surface shaft into the sub. It is desirable to have the control surface far from the center of gravity since the larger the moment arm is, the larger the force generated is, and therefore the smaller control surface size can be reduced which will help reduce skin friction drag.

The actuating rod thickness is an important parameter which determines the final control surface thickness, since the shaft must be small enough to fit within the center of pressure of the control surface cross section in order to get the no resistive torque benefits. The control surface shaft also should be thick enough to allow space for drilled holes for mounting. The controls group thought a diameter of 3/8" was the lowest thickness shaft they were able to drill into.

Since a shaft goes into the control surface the control surface must have a hole drilled into it. Therefore the thickness of control surface around the shaft needs to be known. The estimated spacing requirement around the control shaft hole from the controls given manufacture difficulty was set from an 1/8" to a 1/4".

A limit to what was considered a small angle of actuation was also determined. If actuation angles go over 15 degrees the control surface is typically considered a brake. Therefore, the max value of actuation was set to be below or equal to 15 degrees.

The water temperature of the Carderock basin which is used for the Reynolds number, dynamic viscosity, and water density calculation was approximated for June as being 65 degrees Fahrenheit.

Finally, the mach number was set to 0 since compressibility is minuscule in water.

Xfoil requires inputs for mach number, AOA, and Reynolds number and outputs the Cl, Cd and L/D for given airfoil. From the table of constraints, the mach number was assumed equal to zero and the AOA was set to a maximum of 15 degrees. However, the Reynolds number based off the conditions of the water in the Carderock towing basin needs to be determined. The Reynolds number calculation, shown in Eq.1 below, requires the of density of the water in the Carderock Tow Basin, the expected velocity of the fluid/submarine, the length of the submarine, and the dynamic viscosity of the water. Assuming freshwater at 65 degrees Fahrenheit, rho is equal to 998.51 kg/m^3. The velocity of the submarine determined from our goal design speed is 8.5 kts or 4.37 m/s, the length of the sub is approximately 2.6416 m and the dynamic viscosity of freshwater at 65 degrees Fahrenheit is 0.435 N*s/m^2. Plugging these values in we get a final Reynolds number of approximately 26467.5 as shown below in Eq.1.

$$Re = \frac{\rho V L}{\mu} = \frac{998.51 * 4.37 * 2.6416}{0.4355} = 26467.5 \tag{1}$$

2.2 Xfoil Investigation Procedure

The cross-section design investigation was conducted in Xfoil, an interactive airfoil design program commonly used for the design and analysis of subsonic airfoils. Xfoil utilizes an interactive interface which allows users to modify airfoil geometries and run airfoil performance calculations based off the program's computational model which uses wake permit modelling of viscous layer influences on potential flow (Drela). Xfoil was chosen for this design investigation because it allows the designer to quickly test airfoil models, vary design parameters and develop a reasoning based off these design findings (Drela). For this investigation a low Reynolds number viscous flow analysis was run on several NACA 00 series airfoils. The performance data results from this investigation were then compiled into several plots where different the performance data was analyzed and a final airfoil cross section shape for the control surfaces was determined.

One desirable parameter of the final airfoil cross section is that it has low drag and high lift. The relationship between these two forces can be measured by analyzing an airfoil's L/D ratio, which is a relative measurement of the airfoil's lift to drag efficiency, or aerodynamic efficiency. A test was run to compare the L/D ratio's between a range of NACA 00 series airfoils, ranging from NACA 0007-0024, at AOA's of 0-20 degrees. Note that the last two digits of the NACA 00 number represent the maximum thickness percentage located at 30 percent of the airfoil's chord length from the leading edge of the airfoil, ie 07 for a NACA 0007 represents a 7 percent maximum airfoil thickness at the 30 percent chord length of the airfoil from the leading edge, LE. The range of airfoils tested in Xfoil began at NACA 0007 airfoil, since a test was run on the NACA 0001-0006 airfoils which resulted in a non-converged flow, and this range was extended to a NACA 0024 to see if there were any advantages to having a thick airfoil at higher AOAs.

The Xfoil results from the range of NACA 0007-0024 airfoils tested were then compared to one another using the Xfoil computed performance characteristics such as Cl, Cd and L/D ratio. This process was streamlined using a generated MATLAB code, polar_tablemaker_ugr_2020.m, which initializes a set of user inputted variables into Xfoil and then runs the Xfoil application multiple times for each airfoil, 0007 to 0024, to reduce the amount of time the user spends in the Xfoil

interface. Variables such as the NACA airfoil number, Reynolds number, mach number as well as a sequence of AOAs to test each airfoil at can all be user-defined in this MATLAB script. When run, MATLAB will call Xfoil to conduct a viscous flow analysis on the user-inputted airfoil geometries, calculate their performance details one-by-one, and then store the polar values for: alpha, coefficient of lift, coefficient of drag, pressure drag coefficient, moment coefficient, transition location along the top of the airfoil, and transition location along the bottom of the airfoil in the MATLAB script. This code then outputs plots for AOA vs. Cd, AOA vs. Cl, AOA vs. L/D, and a line plot superimposed on a bar chart comparing the average and maximum L/D for all the airfoil numbers tested on a single plot. Results from this code are shown in the results presentation section further below in this report. For clarity, only the highest six coefficient of lift producing airfoils were plotted. Since the MATLAB code calls upon Xfoil, this code requires the user to have the Xfoil application downloaded.

2.3 Comparison to Constraints

The results from the bar chart produced by polar_tablemaker_ugr_2020.m comparing average and maximum L/D for all the airfoil numbers tested was used to identify three airfoil cross section profiles: the highest maximum L/D ratio airfoil, highest average L/D ratio airfoil, and best compromise between average and maximum L/D ratio airfoil. These parameters were decided as being the best airfoil characteristics because a high L/D average would provide a high amount of turning force over a range of AOAs, a high maximum L/D airfoil would produce the greatest turning moment, and the airfoil in the middle would be the best compromise between these two characteristics. These three airfoils were then compared to the design constraints established in Table 1 using a constraint_plotter_ugr_2020.m MATLAB code which was generated to visually determine which NACA 00 airfoil geometries would be able to house the control surface actuating hole and exterior hole spacings.

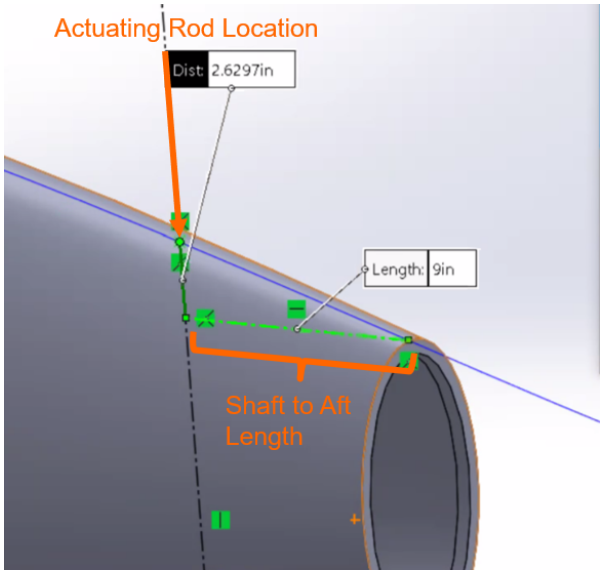

Figure 7: Location of the Shaft and Shaft to Aft Length from SolidWorks

Before any of the airfoil geometries could be plotted, the chord length of the airfoils had to be

determined based off the limited space from the control surface shaft hole to the aft of the submarine. Assuming that the control surface is a single actuating flap which extends from the actuating shaft location to the aft of the submarine, the chord of the control surface from 1/4 chord shaft hole to the airfoil TE is limited to 9", see Fig. 7 above. Therefore the entire chord of the control surface is 9*(5/4)" = 11.25", the 9" is multiplied by 5/4 since the actuating shaft is located at the 1/4 chord of the airfoil, therefore the 9" represents only 3/4" of the airfoil and the other 1/4 of the control surface exists in front of the actuating shaft.

Once the shaft location along the chord of the airfoil was determined, this input, as well as inputs for the shaft hole radius and the upper and lower shaft exterior hole spacing radii were put into the constraint_plotter_ugr_2020.m MATLAB code. This MATLAB code scales and graphs the four user-inputted airfoil geometry profiles to a user defined chord length and then plots the fixed constraint shaft hole, as well as the constraints for the upper and lower bound values of the exterior hole spacing on a single outputted plot. The graphed airfoil profiles allow the designer to visually examine which airfoils meet the soft and hard design constraints. Finally, the code marks a blue cross on the mean aerodynamic center, abbreviated as m.a.c. and also known as the center of pressure, location of the airfoil and plots a blue dashed line indicating the distance of the 1/4 chord from the leading edge, LE. These blue markers act as a verification which allows the user to make sure the shaft hole is centered on the m.a.c. and that the m.a.c is located at the 1/4 chord. This code does not call on Xfoil, therefore the user must have each of the geometry profiles that are desired to be plotted downloaded as "selig" coordinate files. Selig coordinate files list airfoil coordinates starting at the TE and go counter clockwise around the airfoil profile until the TE is reached once more. Results from this code are shown in the analysis of results section under comparison to constraints shown further below in this report.

3 Results Presentation

Figures 8-11, below, show the outputs from the polar_tablemaker_ugr_2020.m airfoil performance characteristic code.

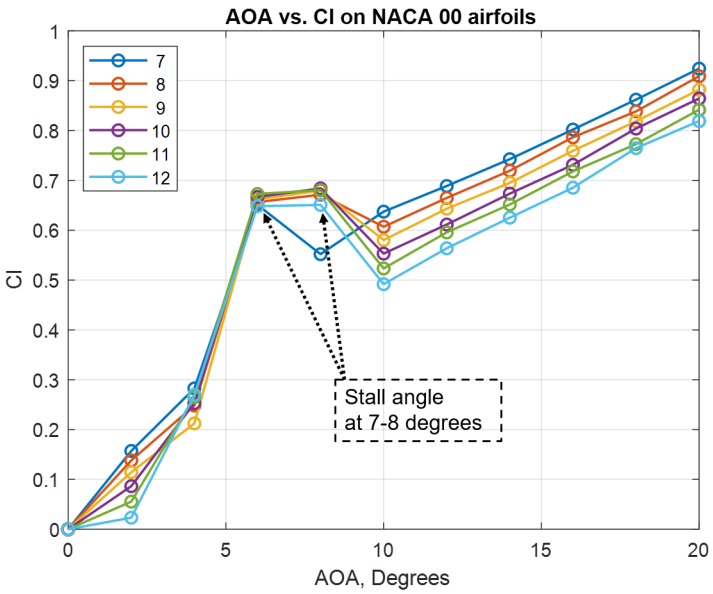

Figure 8: AOA vs. Cl on NACA 00 Airfoils

Figure 8, above, shows the relationship between AOA and Cl on several NACA 00 series airfoils. For clarity, only the highest 6 coefficient of lift producing airfoils were plotted, those being the NACA 0007-12. The AOA varies from 0-20 degrees on the x-axis, and the Cl is shown on the y-axis. The trend shows Cl increases as AOA increases, until the stall angle is met which is 7 degrees for the NACA 00 07 and 8 degrees for the NACA 00 08-12, as shown by the arrows on the plot. This was different than the assumption set earlier which stated the stall angle would be at 15 degrees. There is a noticeable sharp drop in Cl after the AOA passes the stall angle, though further past this stall angle the Cl begins to rise again. One area of future research is why this plot continues to increase after the sharp decline in Cl experienced after the stall angle.

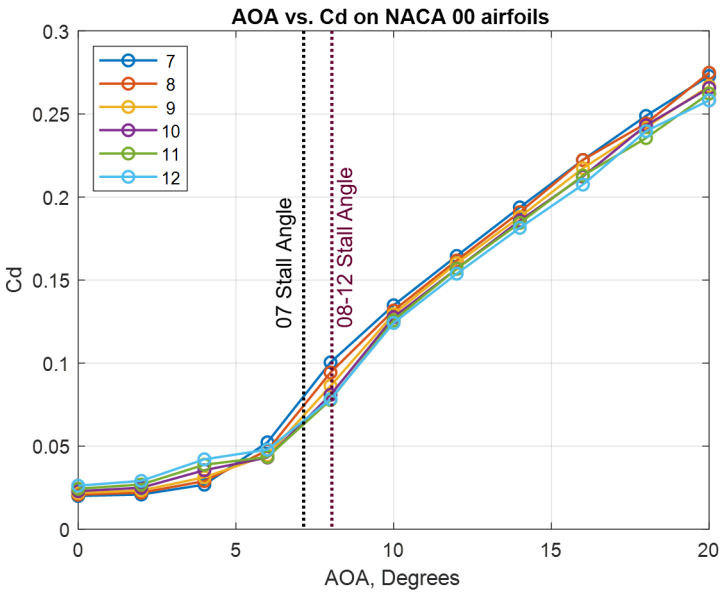

Figure 9: AOA vs. Cd on NACA 00 Airfoils

Figure 9 shows the AOA vs. Cd on NACA 00 airfoils. The same 6 airfoils were plotted over the 0-20 degree range of AOAs as shown in Fig.8. The general trend shows that Cd increases as AOA increases. The Cd trend begins as a gradual increase which eventually transitions into a steeper increase around the stall angle where the drag coefficient ramps up. The stall angles are marked for the different airfoils on the figure where they are shown as vertical dashed lines.

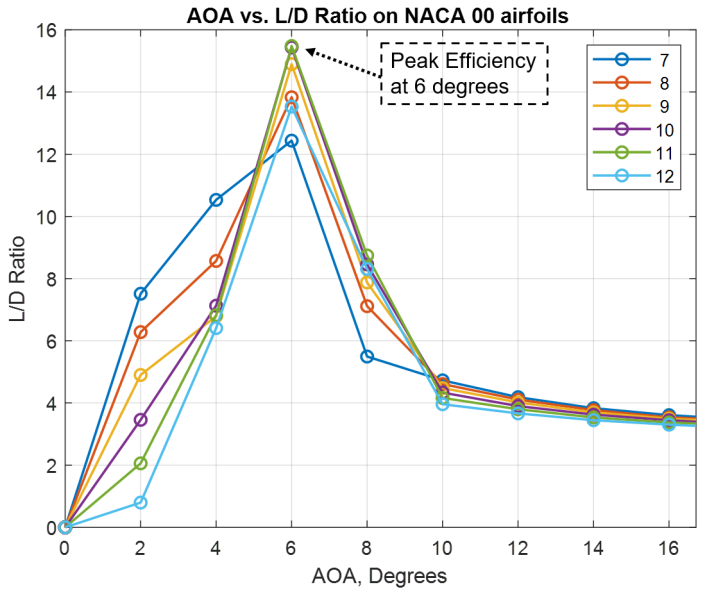

Figure 10: AOA vs. L/D Ratio on NACA 00 Airfoils

Figure 10 shows the AOA vs. L/D ratio on the same 6 NACA 0007-12 airfoils. The plot shows that L/D ratio increases to a peak angle at 6 degrees, marked by an arrow on the diagram, then

decreases afterwards. This reveals the most aerodynamically efficient angle for this range of 0-20 degrees is at 6 degrees. At this 6 degree angle the NACA 0011 is revealed as having the highest max L/D ratio, followed suit by NACA 0010 and 0009. Therefore, at a 6 degree AOA the NACA 0011 is capable of producing the largest turning force of any the airfoils examined in this cross-section investigation.

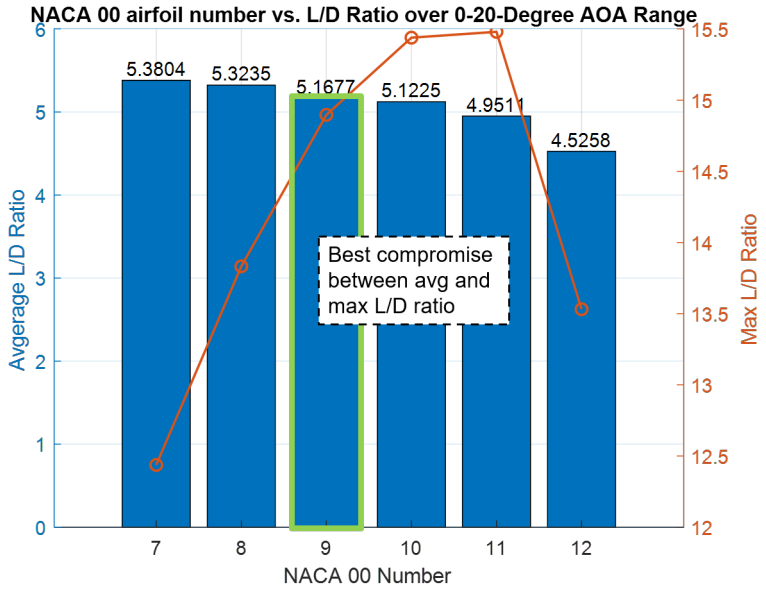

Figure 11: NACA 00 airfoil number vs. L/D Ratio over 0-20 Degree AOA Range

A high aerodynamic efficiency at a specific angle of attack is an important parameter to consider when examining airfoil cross-sectional shapes. Though for an airfoil that will be actuated through a range of attack angles, another important parameter is the average L/D ratio over a specified range of attack angles. A control surface with a high average L/D ratio over a range of AOAs shows the surface as being capable of generating significant turning forces at multiple angles. Figure 11 plots the average and maximum L/D ratio for the same 6 NACA 0007-12 airfoils over the 0-20 degree AOA range as shown by the bar chart and orange line plot respectively. The bar chart shows the smaller maximum thickness percentage NACA airfoils as having a larger average L/D ratio over the 0-20-degree AOA range. If we consider purely average aerodynamic efficiency the NACA 0007 has the highest average L/D ratio.

The Maximum L/D ratio trend allows for a comparison of each airfoils maximum aerodynamic force value, shown by the orange line plot and axis. The NACA 0011 has the highest maximum L/D ratio as shown on the orange line plot. If we consider purely maximum aerodynamic efficiency the NACA 0011 has the highest maximum L/D ratio. Ideally, a control surface would exhibit both a high average and maximum aerodynamic efficiency to provide the pilot with the largest amount of control authority of the vehicle. The best compromise between maximum aerodynamic efficiency and average aerodynamic efficiency is the NACA 0009 as highlighted in green on Figure 11.

4 Analysis of Results

4.1 Verification of Xfoil Results

A verification of the Xfoil results was done by comparing NACA 0012 airfoil results collected from Xfoil to experimental airfoil performance results from *Theory of Wing Sections* by Abott and Doenhoff, see Fig.12. The same inputs were used in Xfoil as were used in the experiment conducted by Abbot and Doenhoff to create an appropriate comparison basis between the Xfoil and experimental results. A NACA 0012 data set tested at a Reynolds number of $9.0*10^2$ from Abott and Doenhoff's experiment, Fig.12 left, was chosen to compare to the same inputs run in Xfoil, Fig.12 right. This Reynolds Number was chosen because the plotted data was one of the more easily readable trends from the Cl and Cd vs. AOA plot produced by Abott and Doenhoff. The Cl and Cd were plotted for a range of AOA varying from -20 to 20 degrees to match the scaling of Abbot and Doenhoff's data.

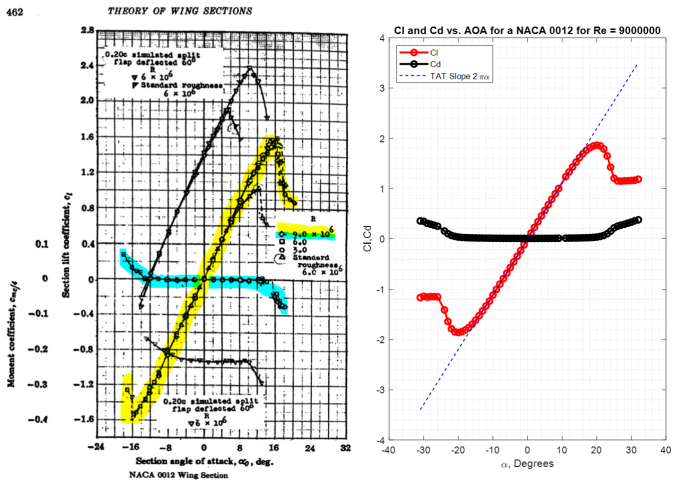

Figure 12: Verification of Xfoil Results, with theoretical values shown (left) (Abbot and Van Doenhoff) and Xfoil results shown (right)

The Theory of Wing Sections Cl and Cd plot vs. AOA is on the left, where the Cl and Cd results are highlighted in yellow and cyan respectively for a Reynolds number of $9.0*10^2$. The Xfoil NACA 0012 airfoil at a Reynolds number of $9.0*10^2$ result is on the right, where the Cl is displayed in red and the Cd in black. The two plots display a similar "S-shaped" for Cl vs. AOA as shown by the yellow and red trends on the theory and Xfoil plots respectively. For Cd vs. AOA, the experimental Cd plot follows an "S-shaped" trend, shown in Cyan, while the Xfoil result differs by displaying a "U-shaped" trend shown in black. Another difference is that there appears to be a deviation in the stall angle between the two plots. For the experimental data, the stall angle is located at an AOA of 16 degrees while on the Xfoil plot it is at 19 degrees. There is also a difference in Max Cl, which peaks at a magnitude of 1.6 on the experimental values plot versus 1.8 on the Xfoil plot. Similarly, a difference in Max Cd is also present which peaks at a magnitude of 0.3 on the experimental values plot versus 0.4 on the Xfoil plot. Why these results vary slightly could be an area of future work, however the overall trends appear to be the same.

4.2 Visualization of Constraints

Figure 13, below, shows the output discussed from the constraint_plotter_ugr_2020.m constraint verification code.

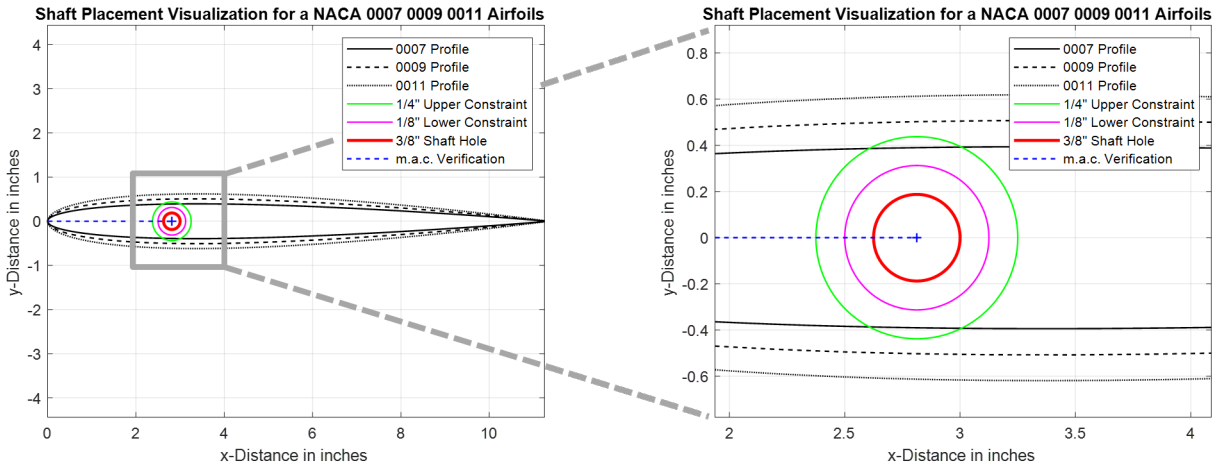

Figure 13: Shaft Placement Visualization for NACA 00 07, 09, and 11 Airfoils

The left side of Fig.13 shows a zoomed out visualization of the three airfoils chosen for having the the highest maximum L/D ratio, highest average L/D ratio, and best compromise between average and maximum L/D ratio plotted against one another. This figure allows for an examination of the airfoils' variation in maximum thickness at the 30 percent chord location to be made. The blue dashed line and the blue cross, the 1/4 chord distance and the m.a.c. location, marked on the figure also act as a verification to make sure the shaft hole is centered on the m.a.c. and that the m.a.c is located at the 1/4 chord. The right side of Fig.13 is the same plot as the plot on the left side of Fig.13 but is enlarged so that the compliance of these airfoils' to the 3/8" shaft diameter hard constraint and the 1/8"-1/4" shaft exterior hole spacing can be more easily examined. It can seen that all three of the airfoil profiles meet the 3/8" shaft hole and 1/8" shaft exterior hole spacing, however only the NACA 0009 and the NACA 0011 airfoils meet the 1/4" shaft exterior hole spacing constraint.

5 Conclusion

It was determined that the NACA 65 66 series airfoils would not be examined since the actuation range of these airfoils is limited to a small range of angles which perform best at high speeds. Since *Nautilus* will be travelling at low speeds the NACA 00 series of airfoils was chosen. The NACA 00 series of airfoils also work well under a wider range of angles which will provide the pilot more autonomy with the control surface actuation range.

The control rod shaft will be placed at the center of pressure of the airfoil to prevent resistive torque which would make the control surface harder to actuate.

The aspect ratio of the control surface geometry should be large, the taper ratio should ideally be between 0.6-0.8, and the span of the control surfaces should lie within the plane of reflection of the hull if possible to mitigate interference of the surfaces with the turbulent boundary layer produced by the hull.

A NACA 00 series airfoil with a high average and maximum L/D ratio is desirable to ensure that the control surface is able to generate sufficient maximum and average turning forces to correct perturbations to the submarine motion. The NACA 0009 was determined as the best option out of the 0007-0024 airfoils tested since it was shown as being the best compromise between the average and maximum L/D ratio and it passes all the design constraints assuming a 9" shaft to aft length.

6 Future Work

Future work consists of looking into possible reason for why there is a rise in the Cl vs. AOA plot after the stall angle is reached. Another area of future work would be to determine possible reasons for the small variations between the results produced by Xfoil and those from *Theory of Wing Sections*. Additionally, future work should continue to iterate control surface geometries as new findings arise and to examine airfoil performance results from the same 0007-0024 NACA 00 airfoils run in Xfoil but at a range of Reynolds Numbers to determine if there are significant differences in any of the hydrodynamic performance characteristics.

References

[1] Abbot and Van Doenhoff. *Theory of Wing Sections*, Dover Publications, Inc. New York, 1959

[2] NASA. "Aerodynamic center - ac", Glenn Research Center, accessed: 2020, May 12, available at: *https://www.grc.nasa.gov/www/k-12/airplane/ac.html*

[3] *"OMER 11 Final Design Report,"* International Submarine Races, accessed: 2020, May 12, available at: *https://internationalsubmarineraces.org/wp-content/uploads/2020/02/OMER-11-DESIGN-REPORT.pdf*

[4] *"Wassub IX Design Report,"* International Submarine Races, accessed: 2020, May 12, available at: *https://internationalsubmarineraces.org/wp-content/uploads/2020/02/Design-report-WASUB-IX-FINAL.pdf*

[5] Drela. *"User Guide in Plain Text"*, MIT Aero and Astro, November 2001

[6] Molland and Turnock. *Marine Rudders and Control Surfaces: Principles, Data, Design and Applications*, Elsevier Ltd., 2007

7 Appendix

7.1 Appendix A: PDF versions of polar_tablemaker_ugr_2020.m and constraint_plotter_ugr_2020.m MATLAB Codes

Table of Contents

Table Maker Code // AUTHOR: Tyler Ellis // LAST EDIT: 5/12/2020

```
%stores the NACA values for alpha, cl, cd, cdp, cm, topxtr, and botxtr
 in
%separate tables for multiple angles of atacks for multiple airfoils.
 The
%each column represnts an airfoil number, each row represents an AOA
%NOTE: if the code fails it is likely due to flow convergence not
 being
%acheived, in such a case try decreasing the resolution of your inputs
clear;
clc; close all;

NACAmin       = '07'; %specify the starting NACA 00'XX' digit airfoil
NACAmax       = '12'; %specify the ending NACA 00'XX' digit airfoil
aseq       = '0 20 2'; %firstangle lastangle spacingbetweenangles

reynoldNum = '26523.8'; %reynolds number
numNodes   = '200'; %number of panels discretized on the airoil
iter = '500'; %number of iterations xfoil does before giving up
mach = '0'; %mach number
saveFlnmAF = 'Save_Airfoil.txt'; %saves polars from xfoil
runs = (str2num(aseq(3:4))-(str2num(aseq(1))))/(str2num(aseq(6)));%#
 of runs from aseq

j=0;i=0;
stop=str2num(NACAmax)-str2num(NACAmin);

    Talpha = zeros(runs+1,stop);%polar tables
    Tcl = zeros(runs+1,stop);
    Tcd = zeros(runs+1,stop);
    Tcdp = zeros(runs+1,stop);
    Tcm = zeros(runs+1,stop);
    Ttop = zeros(runs+1,stop);
    Tbot = zeros(runs+1,stop);

while i<=stop

    countnum=str2num(NACAmin)+j;%iterates NACA00##
    countstr=num2str(countnum);
```

```
    insert='00';
    NACA=strcat(insert,countstr);

    %Delete files if they exist
    if (exist(saveFlnmAF,'file'))
        delete(saveFlnmAF);
    end

    %Create the airfoil
    fid = fopen('xfoil_input.txt','w');
    fprintf(fid,['NACA ' NACA '\n']);

    %Set Parameters
    fprintf(fid,'OPER\n');%enter the operation menu
    fprintf(fid,['iter ' iter '\n']);%sets the iteration limit
    fprintf(fid,['visc ' reynoldNum '\n']); %sets viscous flow &
 inputs reynolds #
    fprintf(fid,['seqp''\n']); %toggle on plot of polar values
%   fprintf(fid,['Mach ' mach '\n']); mach # assumed zero if not
 inputted
    fprintf(fid,['pacc' '\n']); %take the polars
    fprintf(fid,['Save_Airfoil.txt\n\n']);%set a polar file and
 decline writing to save or dump file
    fprintf(fid,['Aseq ' aseq '\n']); %inputs the range of AOAs
    fprintf(fid,['PLIS' '\n']); %show the stored polars while running

    %Close file
    fclose(fid);

    %Run XFoil using input file
    cmd = 'xfoil.exe < xfoil_input.txt';
    [status,result] = system(cmd)

    % READ DATA FILE: AIRFOIL

    saveFlnmAF = 'Save_Airfoil.txt';
    fidAirfoil = fopen(saveFlnmAF);

    dataBuffer = textscan(fidAirfoil,'%f32 %f32 %f32 %f32 %f32 %f32
 %f32','CollectOutput',1,...
        'Delimiter','','HeaderLines',12);

    fclose(fidAirfoil);
    delete(saveFlnmAF);

    %Separate boundary points
    alpha = dataBuffer{1}(:,1); alpha = [zeros(length(runs+1) -
 length(alpha),1),alpha];
    CL = dataBuffer{1}(:,2); CL = [zeros(length(runs+1) -
 length(CL),1),CL];
    CD = dataBuffer{1}(:,3); CD = [zeros(length(runs+1) -
 length(CD),1),CD];
    CDp = dataBuffer{1}(:,4); CDp = [zeros(length(runs+1) -
 length(CDp),1),CDp];
```

```
    CM = dataBuffer{1}(:,5); CM = [zeros(length(runs+1) -
 length(CM),1),CM];
    Top_Xtr = dataBuffer{1}(:,6); Top_Xtr = [zeros(length(runs+1) -
 length(Top_Xtr),1),Top_Xtr];
    Bot_Xtr = dataBuffer{1}(:,7); Bot_Xtr = [zeros(length(runs+1) -
 length(Bot_Xtr),1),Bot_Xtr];
    %Save polar values in a 2D matrix
    Talpha(:,1+j)= alpha;
    Tcl(:,1+j)= CL;
    Tcd(:,1+j)= CD;
    Tcdp(:,1+j)= CDp;
    Tcm(:,1+j)= CM;
    Ttop(:,1+j)= Top_Xtr;
    Tbot(:,1+j)= Bot_Xtr;
    j=j+1;
    i=i+1;
    fprintf(['NACA ',countstr,' of ',NACAmax,'\n']) %shows NACA
 iteration progress
end
```

```
status =
     1
result =
    ''xfoil.exe' is not recognized as an internal or external command,
     operable program or batch file.
     '

Error using textscan
Invalid file identifier. Use fopen to generate a valid file
 identifier.
Error in polar_tablemaker_ugr_2020 (line 71)
    dataBuffer = textscan(fidAirfoil,'%f32 %f32 %f32 %f32 %f32 %f32
 %f32','CollectOutput',1,...
```

PLOT L/D VS. NACA

```
figure ()
length=[str2num(NACAmin):str2num(NACAmax)];
length=transpose(length);%transpose to a column vector
t=numel(length);
Tld=Tcl./Tcd;
% plot3(length(1:t,1),Talpha(:,1:t),Tld(:,1:t),'o','LineWidth',2);grid
 on;
% xlabel('NACA 00 Number')
% ylabel('AOA, Degrees')
% zlabel('L/D Ratio')
plot(Talpha,Tld,'-o','Linewidth',1.25);hold on;
xlabel('AOA, Degrees')
ylabel('L/D Ratio')
title('AOA vs. L/D Ratio on NACA 00 airfoils')
legend(num2str(length));
```

PLOT Avg. L/D VS. NACA # for critical AOAs

```
figure ()
length=[str2num(NACAmin):str2num(NACAmax)];
length=transpose(length);%transpose to a column vector
t=numel(length);
aTld=mean(Tld);
% yyaxis left
bar(length,aTld);grid on;
text(length,aTld,num2str(aTld'),'vert','bottom','horiz','center');
ylabel('Avgerage L/D Ratio')
yyaxis right
p = plot(length,max(Tld),'-o','Linewidth',1.25);
box off
xlabel('NACA 00 Number')
% ylabel('Max L/D Ratio')
title('NACA 00 airfoil number vs. L/D Ratio over 0-20-Degree AOA
 Range')
```

PLOT CL VS. AOA

```
figure ()
length=[str2num(NACAmin):str2num(NACAmax)];
length=transpose(length);%transpose to a column vector
t=numel(length);
plot(Talpha,Tcl,'-o','Linewidth',1.25);grid on;
xlabel('AOA, Degrees')
ylabel('Cl')
title('AOA vs. Cl on NACA 00 airfoils')
legend({num2str(length)},'Location','northwest');
```

PLOT Cd VS. AOA

```
figure ()
length=[str2num(NACAmin):str2num(NACAmax)];
length=transpose(length);%transpose to a column vector
t=numel(length);
plot(Talpha,Tcd,'-o','Linewidth',1.25);grid on;
xlabel('AOA, Degrees')
ylabel('Cd')
title('AOA vs. Cd on NACA 00 airfoils')
legend({num2str(length)},'Location','northwest');
```

Published with MATLAB® R2019a

Constraint Plotter Code // AUTHOR: Tyler Ellis // LAST EDIT: 5/12/2020

```
%plots the profiles of up to four airfoils all at once against the
%design constraints specified by the user. NOTE Xfoil is not called
 upon in
%this code, as a result the 'selig' formatted coordinates of each of
 the airfoils
%used must be downloaded and in your MATLAB directory.
clc
clear all
format compact
close all
% upload airfoil coordinates
NACA1='0007'; upload1=['NACA',NACA1,'.txt'];coords1 =
 importdata(upload1);
NACA2='0009'; upload2=['NACA',NACA2,'.txt'];coords2 =
 importdata(upload2);
NACA3='0011'; upload3=['NACA',NACA3,'.txt'];coords3 =
 importdata(upload3);
NACA4='0011'; upload4=['NACA',NACA4,'.txt'];coords4 =
 importdata(upload4);

shaftfromTE= 9; % in inches = 0.2286 m // length of shaft to TE of
 airfoil
c=shaftfromTE+shaftfromTE*0.25; % in m // calculates chord length of
 airfoil
rsafeMAX=0.4375; %in inches = 0.0111125 m // required spacing radius +
 shaft radius
rsafeMIN=0.3125; %in inches
rShaft= (3/8)/2; % in inches = 0.0047625 m // required shaft hole
 radius

X1=coords1(:,1)*c;%(rows,columns)
Y1=coords1(:,2)*c;
X2=coords2(:,1)*c;
Y2=coords2(:,2)*c;
X3=coords3(:,1)*c;
Y3=coords3(:,2)*c;
X4=coords4(:,1)*c;
Y4=coords4(:,2)*c;

%%%%%%%%%%%%%%%%%%%%%%%%%%%%%%%%%%%%%%%%%%%%%%%%%%%%%%%%%%%%%%%%%%%%%%%%%%%%%%%

Error using importdata (line 139)
Unable to open file.
Error in constraint_plotter_ugr_2020 (line 11)
NACA1='0007'; upload1=['NACA',NACA1,'.txt'];coords1 =
 importdata(upload1);
```

PLOT All Airfoils and Constraints

```
figure()
plot(X1, Y1, 'k-','LineWidth', 1); hold on;
axis equal; grid on;
plot(X2, Y2, 'k--','LineWidth', 1); hold on;
axis equal; grid on;
plot(X3, Y3, 'k:','LineWidth', 1); hold on;
axis equal; grid on;
% plot(X4, Y4, 'k-.','LineWidth', 1); hold on;
% axis equal; grid on;

%SPACING HOLE safeMAX
x=rsafeMAX;
y=0;
th = 0:pi/100:2*pi;
xunit1 = rsafeMAX * cos(th);
yunit1 = rsafeMAX * sin(th);
plot(xunit1+(0.25*c), yunit1,'g','LineWidth',1);hold on;
%SPACING HOLE safeMIN
x2=rsafeMAX;
y=0;
th = 0:pi/100:2*pi;
xunit2 = rsafeMIN * cos(th);
yunit2 = rsafeMIN * sin(th);
plot(xunit2+(0.25*c), yunit2,'m','LineWidth',1);hold on;
%SHAFT HOLE
x=rsafeMAX;
y=0;
th = 0:pi/100:2*pi;
xunit3 = rShaft * cos(th);
yunit3 = rShaft * sin(th);
plot(xunit3+(0.25*c), yunit3,'r','LineWidth',2);hold on;

% %verification of the TE to shaft hole length
% x=[0.25*c c]; y=[0 0];
% plot(x,y,'--c','LineWidth',1);hold on;

% %verification the mac passes through the shaft hole
x4=[0 0.25*c]; y4=[0 0];
plot(x4,y4,'--b','LineWidth',1);hold on;

%marks the shaft hole centroid (at the mean aerodynamic center!)
x5=[0.25*c]; y5=[0];
plot(x5,y5,'b+','LineWidth',1);hold on;

title(['Shaft Placement Visualization for a NACA ',num2str(NACA1),'
 ',num2str(NACA2),' ',num2str(NACA3),' ','Airfoils'])
xlabel('x-Distance in inches')
ylabel('y-Distance in inches')
legend([num2str(NACA1),' Profile'],[num2str(NACA2),' Profile'],
[num2str(NACA3),' Profile'],'1/4" Upper Constraint', '1/8" Lower
 Constraint','3/8" Shaft Hole','m.a.c. Verification')
```